Adv. Geom. **10** (2010), 587–602
DOI 10.1515/ADVGEOM.2010.033

Advances in Geometry

Triply periodic minimal surfaces which converge to the Hoffman–Wohlgemuth example

Plinio Simões and Valério Ramos Batista*

(Communicated by K. Ono)

Abstract. We get a continuous one-parameter new family of embedded minimal surfaces, of which the period problems are two-dimensional. Moreover, one proves that it has Scherk's second surface and Hoffman–Wohlgemuth's example as limit-members.

1 Introduction

A continuous family $\mathcal{F}$ of complete embedded minimal surfaces can play an important role in the development of their global theory. One of the most beautiful examples is *the genus one helicoid*, which turned out to be a second example of complete minimal submanifold of $\mathbb{R}^3$ *with only one end*, besides the helicoid. To date, one has not found any further examples of this kind yet. For details, see [2], [8] and [18].

Sometimes, one can find $\mathcal{F}$ enclosing all surfaces of a certain class. For instance, in 2005 Pérez, Rodríguez and Traizet proved that any doubly periodic minimal torus with parallel ends is an interior point of a cube $\mathcal{F}$ (see [14]). Such families are essential to understand the moduli space of minimal surfaces.

At this point, we remark that the above references deal with *two-dimensional* period problems. By this concept we do not count López–Ros parameters, and that dimension has been the highest in which one succeeds in finding a non-trivial *explicit* $\mathcal{F}$. To date, there still remain only few such examples, while many $\mathcal{F}$'s were obtained from *one-dimensional* period problems (see [3], [5], [7], [6] and [16]).

By the way, [16] builds a strong parallel to this present work, for there one proves that Scherk's second surface and Callahan–Hoffman–Meeks' [1] are limit-members of a *unique* $\mathcal{F}$, in the sense that it encloses all the examples presented therein. In this paper we show that handle addition is possible for that *whole* $\mathcal{F}$, with one limit-member being an example from Hoffman and Wohlgemuth (see [4] and [17]).

*This work was supported by FAPESP grant numbers 00/07090-5, 01/05845-1 and 05/00026-3.

If one seeks after a new isolated surface with less than three period problems, then handle addition is an old and widely known technique, though not always successful. In this work, however, we not only present a full study of a continuous family of new surfaces, but also do it practically *without* computations. Instead, geometric arguments are intensively used, many of them profiting from former results like [10] and [16]. By studying periods, one takes homotopic curves based on a *best-choice* procedure, detailed in Section 6.

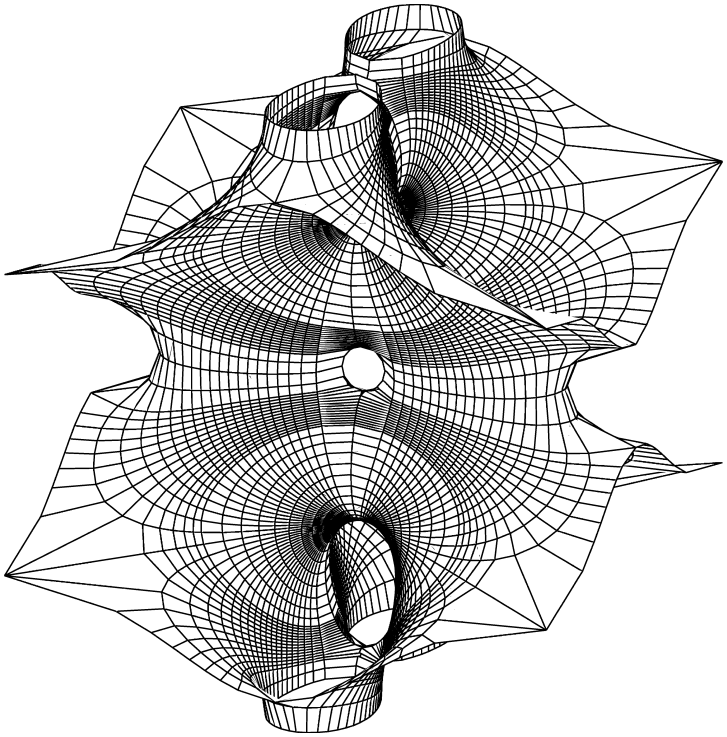

Figure 1. Fundamental piece of a triply periodic Costa surface with handles.

Let us first consider Figure 1. The main goal of this paper is then to prove the following:

Theorem 1.1. *There exists a one-parameter family of complete triply periodic minimal surfaces in* $\mathbb{R}^3$ *such that, for any member of this family the following holds:*

(a) *The quotient by its translation group* G *has genus* 7.

(b) *The whole surface is generated by a fundamental piece, which is a surface with boundary in* $\mathbb{R}^3$. *The boundary consists of eight planar curves of vertical reflectional symmetry and four planar curves of horizontal reflectional symmetry. The fundamental piece has a symmetry group generated by two vertical planes of reflectional symmetry and two line segments of* 180°*-rotational symmetry.*

(c) *By successive reflections in the boundary of the fundamental piece one obtains the triply periodic surface.*
(d) *All members in the family are embedded in* $\mathbb{R}^3$. *Moreover, it has two limit-members: the Hoffman–Wohlgemuth example of genus* 5 *and two side-by-side copies of Scherk's doubly periodic surface.*

Now we state a consequence of Theorem 1.1:

Corollary 1.1 (Hoffman–Wohlgemuth surface). *There exists an embedded singly periodic minimal surface in* $\mathbb{R}^3$ *with the following properties:*

(a) *The quotient by its translation group has genus* 5.
(b) *This quotient has two planar ends, and a symmetry group generated by two vertical planes of reflectional symmetry and two straight lines of* 180°*-rotational symmetry.*

The proof of Corollary 1.1 will be discussed at the end of Section 8. Such a result will follow in a much easier fashion than in [17], due to Theorem 1.1.

2 Preliminaries

In this section we state some basic definitions and theorems. Throughout this work, surfaces are assumed to be connected and regular. Details can be found in [6], [9], [12] and [13].

Theorem 2.1. *Let* $X : R \to \mathbb{E}$ *be a complete isometric immersion of a Riemannian surface* R *into a three-dimensional complete flat space* $\mathbb{E}$. *If* X *is minimal and the total Gaussian curvature* $\int_R K\, dA$ *is finite, then* R *is biholomorphic to a compact Riemann surface* $\overline{R}$ *punched at a finite number of points.*

Theorem 2.2 (Weierstrass representation). *Let* R *be a Riemann surface,* g *and* dh *meromorphic function and* 1*-differential form on* R*, such that the zeros of* dh *coincide with the poles and zeros of* g. *Suppose that* $X : R \to \mathbb{E}$*, given by*

$$X(p) := \operatorname{Re} \int^p (\varphi_1, \varphi_2, \varphi_3), \quad \textit{where} \quad (\varphi_1, \varphi_2, \varphi_3) := \frac{1}{2}(g^{-1} - g, ig^{-1} + ig, 2)\, dh,$$

is well-defined. Then X *is a conformal minimal immersion. Conversely, every conformal minimal immersion* $X : R \to \mathbb{E}$ *can be expressed as above for some meromorphic function* g *and* 1*-form* dh.

Definition 2.1. The pair (g, dh) is the *Weierstrass data* and φ_1, φ_2, φ_3 are the *Weierstrass forms* on R of the minimal immersion $X : R \to X(R) \subset \mathbb{E}$.

Theorem 2.3. *Under the hypotheses of Theorems* 2.1 *and* 2.2*, the Weierstrass data* (g, dh) *extend meromorphically on* $\overline{R}$.

The function g is the stereographic projection of the Gauss map $N : R \to S^2$ of the minimal immersion X. It is a covering map of $\hat{\mathbb{C}}$ and $\int_S KdA = -4\pi \deg(g)$. These facts will be largely used throughout this work.

3 The symmetries of the surface and the elliptic Z-function

Let us consider Figure 1, which represents the fundamental piece of a triply periodic surface S. If G denotes its translation group, then S/G is a compact Riemann surface of genus 7 that we call $\bar{S}$ (see Figure 2(a)). Let ρ be the map from $\bar{S}$ to its quotient by 180°-rotation around the x_3-axis. Then, the Euler–Poincaré characteristic of $\rho(\bar{S})$ is given by $\chi(\rho(\bar{S})) = \frac{1}{2}\chi(\bar{S}) + 6 = 0$. Because of this, $\rho(\bar{S})$ is a torus that we call T. This torus must be rectangular because of the following argument. The horizontal reflectional symmetries of $\bar{S}$ are inherited by T through ρ, and there are two curves which remain invariant under any of these symmetries. Then, the fixed-point set has two components and this only happens for the rectangular torus.

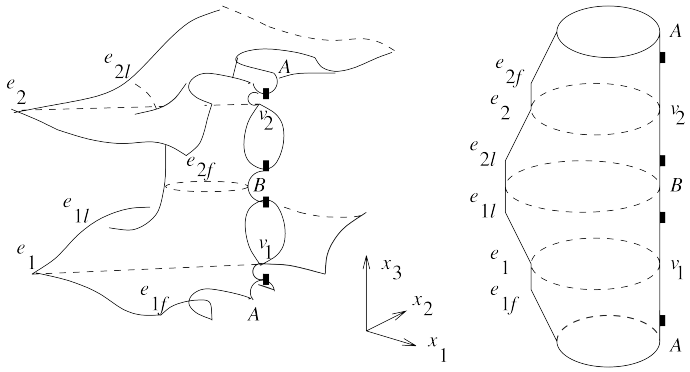

(a) (b)

Figure 2. (a) Half of $\bar{S}$; (b) the torus T.

The surface $\bar{S}$ has two other 180°-rotational symmetries, namely the ones around the x_1- and x_2-axes. The torus T has these two symmetries as well. Let r be the 180°-rotational symmetry around the x_1-axis. The quotient of T by r is conformally S^2. After we fix an identification of S^2 with $\hat{\mathbb{C}}$, we finally obtain an elliptic function $Z : T \to S^2$.

Consider Figure 2(b) and the points of the torus T represented there. These correspond to special points of $\bar{S}$, indicated in Figure 2(a) (they were given the same names). Let $Z : T \to S^2$ be the elliptic function with $Z(e_1) = 1/Z(e_2) = 0$ and $Z(v_1) = 1/Z(v_2) = a$, where a is a real value in $(0, 1)$ (these functions coincide with $\cos\alpha \cdot \wp + \sin\alpha$ described in [6, p. 40]).

Now we summarize some important properties of the function Z (see Figure 3). It is real on the bold lines (and nowhere else), and $|Z| = 1$ on the dashed lines (and nowhere else). It has exactly four branch points, marked with $\times$ in Figure 3. At the points A and B the function Z takes the value 1 and at the points C (center) and D, the value -1.

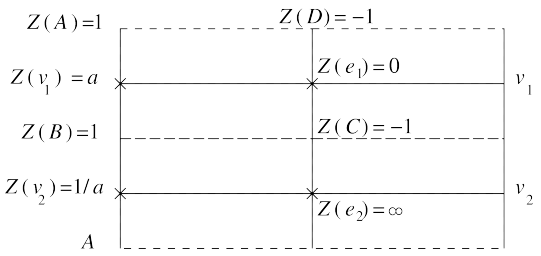

Figure 3. The torus T with values of Z at special points on it.

4 The z-function on $\bar{S}$ and the Gauss map in terms of z

In this section we start by studying the necessary conditions for the existence of a minimal surface like in Figure 1. They will lead to an algebraic equation for the compact Riemann surface $\bar{S}$, together with Weierstrass data on it. From this point on, our problem will be concrete. We shall have to prove that the algebraic equation really corresponds to $\bar{S}$ in terms of its genus and symmetries. Afterwards, we shall have to prove that the Weierstrass data really lead to a minimal embedding of $\bar{S}$ in $\mathbb{R}^3/G$ with the expected properties: symmetry curves, periodicity, etc.

Let us call S the surface represented in Figure 1 and suppose that it is a minimal immersion of $\bar{S}$ in $\mathbb{R}^3/G$. In this case, we make use of the previous section and consider the functions $\rho : \bar{S} \to T$ and $Z : T \to \mathbb{C}$. Let us define $z := Z \circ \rho$. Both functions Z and ρ have degree 2, z is a function on $\bar{S}$ of degree 4 (see Figure 4(a)). In this picture one sees that z takes on special values $b \in (a, 1)$ and $-x \in (-1, 0)$ on $\bar{S}$.

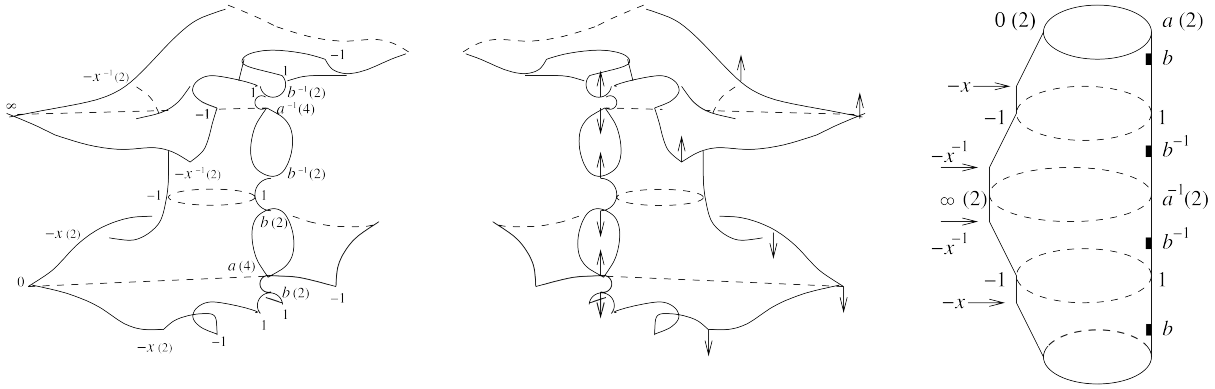

Figure 4. (a) Values of z at special points; (b) The corresponding normal vector at these points; (c) the corresponding values of Z on T.

We are supposing that S is a minimal immersion of $\bar{S}$ in $\mathbb{R}^3/G$. In this case, the Gauss map on S must lead to a meromorphic function g on $\bar{S}$, as Figure 4(b) suggests.

We are going to define *multiplicity* as the branch order plus one. Then, the expected correspondence between the values of z and g (including their multiplicities) is indicated in Figure 4(a) and 4(b). Therefore, one establishes the following relation:

$$g^4 = z\left(\frac{1-az}{z-a}\right)\left(\frac{b-z}{bz-1}\right)^2\left(\frac{z+x}{xz+1}\right)^2. \tag{1}$$

From now on we define $\bar{S}$ as a general member of the family of compact Riemann surfaces given by (1). These surfaces have genus 7, because of the following argument: each value $z \in \{a^{\pm 1}, 0^{\pm 1}\}$ represents 1 branch point of multiplicity 4 on $\bar{S}$, and each value $z \in \{-x^{\pm 1}, b^{\pm 1}\}$ represents 2 different branch points of multiplicity 2 on $\bar{S}$. This function is a four-sheet branched covering of the sphere. Therefore, by the Riemann–Hurwitz formula, the genus of $\bar{S}$ is

$$\frac{4\cdot 1\cdot(4-1)+4\cdot 2\cdot(2-1)}{2} - 4 + 1 = 7. \tag{2}$$

Some involutions of $\bar{S}$ are summarized in Table I. This table includes the differential dh which will be discussed in the next section.

Table I: Involutions of $\bar{S}$.

	involution	z-values	$g \in$	$dh(\dot{z}) \in$
1	$(z,g) \to (\bar{z}, \bar{g})$	$-1 < z < -x$	$\mathbb{R}$	$\mathbb{R}$
2	$(z,g) \to (\bar{z}, -\bar{g})$	$-x < z < 0$	$i\mathbb{R}$	$\mathbb{R}$
3	$(z,g) \to (\bar{z}, \pm i\bar{g})$	$0 < z < a$	$\pm\sqrt{i}\mathbb{R}$	$i\mathbb{R}$
4	$(z,g) \to (\bar{z}, -\bar{g})$	$a < z < b$	$i\mathbb{R}$	$\mathbb{R}$
5	$(z,g) \to (\bar{z}, \bar{g})$	$b < z < 1$	$\mathbb{R}$	$\mathbb{R}$
6	$(z,g) \to (1/\bar{z}, 1/\bar{g})$	$z \in S^1$	S^1	$i\mathbb{R}$

We have just proved that the values of g on all special curves of $\bar{S}$ are consistent with the expected unitary normal on the minimal surface S in $\mathbb{R}^3/G$.

5 The height differential dh in terms of z

Now we need an expression for the differential form dh. The surface has no ends and because of this dh is holomorphic. Its zeros are exactly the ones where $g = 0$ or $g = \infty$ and all have multiplicity 1 (i.e., branch order 0). If we consider the differential form dz, then it would be sufficient to divide it by a function on the surface with double zeros at $z \in \{0, a^{\pm 1}\}$ and a pole of multiplicity 6 at $z = \infty$. This function will turn out to be the pull-back by ρ of another function, that we call V, on the torus T.

Since $0^{\pm 1}$ and $a^{\pm 1}$ are the only branch values of Z, all of them of order one, the torus T can be algebraically described by the equation

$$V^2 = Z(Z-a)(Z-1/a). \tag{3}$$

Now, $V \circ \rho$ has exactly the zeros and poles on $\bar{S}$ with the expected multiplicities. We can take $v := V \circ \rho$. This means that v is a well-defined square root of the function $z(z-a)(z-1/a)$ on $\bar{S}$. For instance, $v/z =: \sqrt{z+1/z-a-1/a}$.

Finally, we need to establish a proportional constant to determine dh by means of dz/v. On the straight lines of the surface, where $0 < z^{\pm 1} < a$, the coordinate $x_3 = \mathrm{Re} \int dh$ must be constant. Then $\mathrm{Re}\{dh\}$ is zero there. Because of this we choose the proportional constant to be i, namely

$$dh = \frac{idz}{v} = \frac{idz/z}{\sqrt{z+1/z-a-1/a}}. \tag{4}$$

At this point we have reached concrete Weierstrass data (g, dh) on $\bar{S}$, defined by (1) and (4), with x, a and b satisfying

$$0 < a < b < 1 \quad \text{and} \quad 0 < x < 1. \tag{5}$$

Now our task will be the demonstration of the following: let S be the minimal immersion of $\bar{S}$ given by these Weierstrass data. Then S leads to the expected surface whose fundamental piece is represented in Figure 1. In other words, we need to show that S really has all the symmetry curves and lines of our initial assumptions, and the fundamental piece of S has *no periods*, as indicated in Figure 1. This second task will be discussed in the next section. Now we analyze the symmetries of S.

From (1) and (4) we see that all the z-curves listed in Table I are geodesics, because $g(z)$ is contained either in a meridian or in the equator of S^2, *and* $dh(\dot{z})$ is contained in a meridian of S^2. Moreover, the geodesics are straight lines if $0 < z^{\pm 1} < a$, because in this case $\frac{dg(\dot{z})}{g(z)} \cdot dh(\dot{z}) \in i\mathbb{R}$. Otherwise we have $\frac{dg(\dot{z})}{g(z)} \cdot dh(\dot{z}) \in \mathbb{R}$ and the corresponding geodesics will be planar. Therefore, S has all the expected symmetries.

6 Solution of the period problems

The triply periodic minimal surface S is generated by its translation group G applied to a fundamental piece. Its right half is shown in Figure 5(a). The fundamental domain for the full symmetry group of the minimal surface is the shaded region represented on Figure 5(a).

Since S has no ends, we need to analyze the period vector given by $\mathrm{Re} \oint (\varphi_1, \varphi_2, \varphi_3)$ on the curves of the homology of $\bar{S}$. This task is very similar to the analysis done in [16, pp. 80–81] and will be skipped here. We conclude that just two period problems remain to be solved, namely

$$\mathrm{Re} \int_\gamma \varphi_2 = 0 \quad \text{and} \quad \mathrm{Re} \int_\delta \varphi_2 = 0, \tag{6}$$

where γ and δ are represented in Figure 5(a). The branches of the square root need to be chosen in accordance with Figures 5(a) and 5(b). This choice is indicated in Figure 6.

The curve γ can be explicitly given by $z(t) = z \circ \gamma(t) = e^{it}, 0 < t < \pi$. If we define $\Gamma := \rho \circ \gamma$, then $Z \circ \Gamma(t) = z \circ \gamma(t)$. We establish the 4^{th}-root on $z(t)$ of each factor in (1) as indicated in Figure 7.

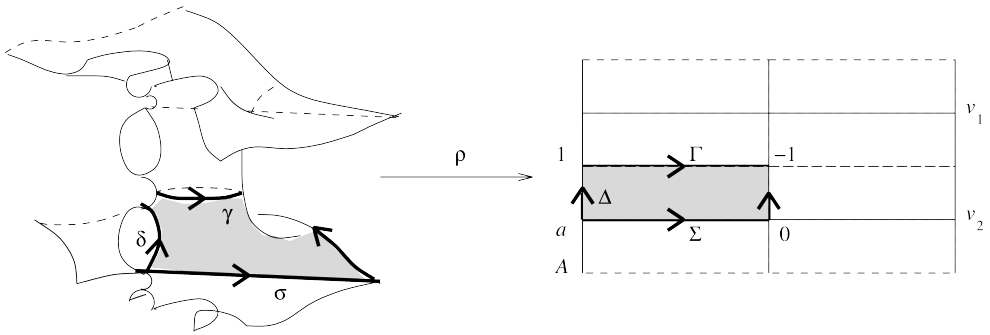

Figure 5. (a) The right half of the fundamental piece; (b) Its corresponding image under ρ.

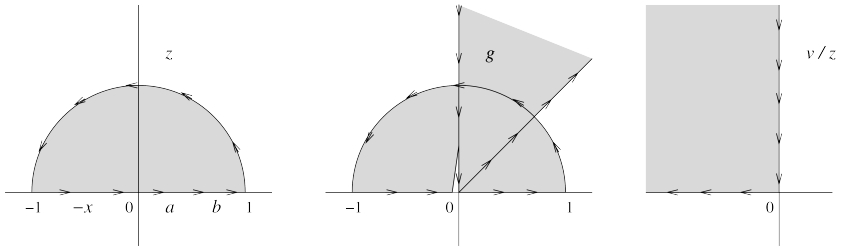

Figure 6. The images of $|z| < 1 < 1 + \mathrm{Im}\{z\}$ under g and v/z.

The condition $\mathrm{Re}\int_\gamma \varphi_2 = 0$ will then be equivalent to

$$\frac{1}{2}\int_0^\pi (g + g^{-1})\,|dh| = \int_0^\pi \mathrm{Re}(g)\,|dh| = 0, \tag{7}$$

where

$$dh = \frac{idt}{\sqrt{a + 1/a - 2\cos t}} \quad \text{and} \quad g = g(z(t)) \in S^1. \tag{8}$$

It is not difficult to see that $\mathrm{Re}(g(t))$ is increasing with x and decreasing with b. Let us now vary b in the interval $(a, 1)$. From *Lebesgue's dominated convergence theorem*, at the extremes we have the following equalities for $I_\gamma := \int_0^\pi \mathrm{Re}(g)\,|dh|$:

$$I_\gamma|_{b=a} = \int_0^\pi \mathrm{Re}\left\{\sqrt[4]{z}\cdot\sqrt[4]{\frac{z-a}{1-az}}\cdot\sqrt{\frac{z+x}{xz+1}}\right\}\frac{dt}{\sqrt{a+1/a-2\cos t}} \tag{9}$$

and

$$I_\gamma|_{b=1} = -\int_0^\pi \mathrm{Im}\left\{\sqrt[4]{z}\cdot\sqrt[4]{\frac{1-az}{z-a}}\cdot\sqrt{\frac{z+x}{xz+1}}\right\}\frac{dt}{\sqrt{a+1/a-2\cos t}}. \tag{10}$$

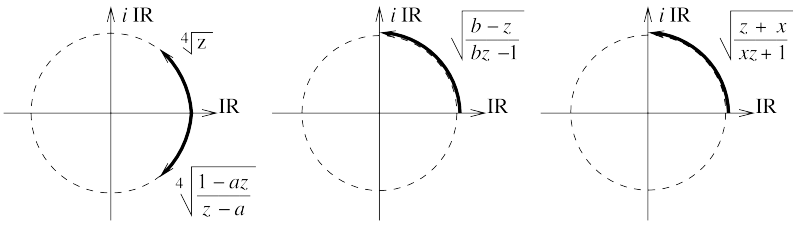

Figure 7. The 4th-roots on $z(t)$ of the factors in (1).

Both functions in (9) and (10) are still increasing with x. Let us analyze the integrand of (10). It is easy to prove that

$$\tan Arg\left\{ z \cdot \frac{1-az}{z-a} \right\} = \frac{2\sin t \cdot (a\cos t - 1)}{a + 1/a}. \tag{11}$$

Hence, at $x = 1$ the integrand of (10) will be always positive. Therefore, $I_\gamma|_{(b,x)=(1,1)} > 0$ for any $a \in (0,1)$. It is not difficult to see that $a^{-1/2} I_\gamma|_{(b,x)=(1,0)}$ is negative for a close to zero, while it diverges to $+\infty$ when a approaches 1. Notice that the factor $\mathrm{Im}\{\cdot\}$ is monotonely decreasing with a. For any fixed $a \in (0,1)$, it changes sign at a certain unique $t_a \in (0,\pi)$. Now consider a value $a = \alpha$ where $I_\gamma|_{(b,x)=(1,0)}$ vanishes. If one takes $p := (1/\alpha - \alpha)/(1/\alpha + \alpha - 2\cos t_\alpha)$, then an easy computation shows that the derivative of $a^{-p/2} I_\gamma|_{(b,x)=(1,0)}$ with respect to a is positive at α. This means that α is the *unique* value of a that makes $I_\gamma|_{(b,x)=(1,0)}$ equals zero. Since the integral at (10) is increasing with x, we have just proved the following:

For any $a \in (0,\alpha)$, there exists a unique $x = x_a$ such that $I_\gamma|_{(b,x)=(1,x_a)} = 0$. If $a \in (\alpha,1)$, then $I_\gamma|_{b=1}$ is always positive. Moreover, $\lim_{a\to\alpha} x_a = 0$.

Let us now analyze the integral at (9). For $x = 0$, it diverges to $+\infty$ when a approaches 1. Take a compact $\mathcal{K} \subset \mathbb{C} \setminus \{0, a^{\pm 1}\}$ such that $S^1 \subset \mathcal{K}$. One easily sees that our data $(1/g, dh)$ converge uniformly in $\mathcal{K}$ to the Weierstrass pair $(\boldsymbol{g}, \boldsymbol{g}\eta)$ from [10, pp. 452–453], for the following choice of parameters defined there: $\boldsymbol{a} = 1/a$, $\boldsymbol{A} = 1$ and $\boldsymbol{B} = i\sqrt{\boldsymbol{a}}$. Therefore, $I_\gamma|_{(b,x)=(a,0)}$ coincides with $\frac{1}{2}\int_{\gamma_2} \boldsymbol{\phi}_2$, where γ_2 is described in [10, p. 455]. There one proves that $\int_{\gamma_2} \boldsymbol{\phi}_2 \neq 0$ for any $\boldsymbol{a} > 1$. Consequently, $I_\gamma|_{(b,x)=(a,0)} > 0$ for all $a \in (0,1)$. Since $I_\gamma|_{b=a}$ is increasing with x, then $I_\gamma|_{b=a} > 0$ on the whole square $(0,1)^2 \ni (a,x)$.

We recall that $\mathrm{Re}\{g(t)\}$ is increasing and decreasing with x and b, respectively. Hence, there is a function $b(a,x)$, defined in the region $\mathcal{R} := \{(a,x) \in (0,1)^2 : x \leq x_a\}$, such that $I_\gamma|_{b=b(a,x)} = 0$ and non-zero elsewhere. Moreover, $b(a,x)$ can be continuously extended to $\partial\mathcal{R}$ and $\lim_{(a,x)\to(0,0)} b(a,x) = 0$. Henceforth in this section, the parameter b will always represent *this* function.

One easily sees that φ_2 is purely imaginary for $-1 < z < -x$ and $b < z < 1$. From Figure 5(b) we get $\mathrm{Re}\int_\delta \varphi_2 + \mathrm{Re}\int_\gamma \varphi_2 = \mathrm{Re}\int_\sigma \varphi_2$. From the above paragraph, the second integral is zero. Therefore, it remains to prove that either $\mathrm{Re}\int_\delta \varphi_2$ or $\mathrm{Re}\int_\sigma \varphi_2$ vanishes for a suitable choice of $(a,x) \in \mathcal{R}$. In order to do it, we shall make use of the following result:

Lemma 6.1. *The above defined α is bigger than $1/2$.*

Proof. Let us take $x = 0$ at (10) and study the imaginary part of the function $z^3(1 - az)/(z - a)$, for $z = e^{it}$, $0 \leq t \leq \pi$. A simple reckoning shows that

$$\mathrm{Im}\left\{\frac{z^3(1/a - z)}{z/a - 1}\right\} = \frac{\sin(2t)/a^2 - 2\sin(3t)/a + \sin(4t)}{(\cos t/a - 1)^2 + \sin^2 t/a}. \tag{12}$$

If $a < 1/2$, the derivative of (12) at either $t = 0$ or $t = \pi$ is positive. Although it vanishes at both extremes for $a = 1/2$, one still concludes that $\mathrm{Im}\{\cdot\}$ is increasing there. For $a = 1/2$, one rewrites the numerator of (12) as $4\sin t(1 - \cos t)(2\cos t - \cos 2t)$. Since $\sin t(1 - \cos t)$ never vanishes in $(0, \pi)$, in this interval there is a single zero at $t = t_0 := \arccos((1 - \sqrt{3})/2)$. The real part of $z^3(1 - az)/(z - a)$ has the same sign of $\cos(2t)/a^2 - 2\cos(3t)/a + \cos(4t)$, which at t_0 takes the value $-2^{\frac{3}{2}} \cdot 3^{\frac{1}{4}} \cdot (2\sqrt{3} - 3)^{\frac{1}{2}} - 4\sqrt{3}$. This means that the argument of $z^3(1 - az)/(z - a)$ varies from 0 to 2π without taking negative values. Therefore, the integral at (10) is negative at $a = 1/2$. □

Now we parametrize the curve δ as $z(t) = z \circ \delta(t) = t, a < t < b$. If $\Delta := \rho \circ \delta$, then $Z \circ \Delta(t) = z \circ \delta(t)$. From Figure 6 we have

$$g(\delta(t)) = i|g(t)| = it^{\frac{1}{4}} \left(\frac{1 - at}{t - a}\right)^{\frac{1}{4}} \left(\frac{b - t}{1 - bt}\right)^{\frac{1}{2}} \left(\frac{t + x}{xt + 1}\right)^{\frac{1}{2}} \tag{13}$$

and

$$dh(t) = |dh(t)| = \frac{dt/t}{\sqrt{a + 1/a - t - 1/t}}. \tag{14}$$

Therefore, $\varphi_2 \circ \delta(t) = (|g|^{-1} - |g|)|dh|$. At the points $(a, x) = (a, x_a)$ we have $b \equiv 1$. Under this condition and from (13), φ_2 will be negative providing

$$a(t^4 - 1) + (x^2 + 2ax - 1)(t^3 - t) < 0. \tag{15}$$

Since $t^2 - 1$ is always negative in $(a, 1)$, then (15) is equivalent to

$$t + 1/t > (1 - 2ax - x^2)/a. \tag{16}$$

A sufficient condition for (16) to hold is that $2a > 1 - 2ax - x^2$. Due to Lemma 6.1, it follows that $\mathrm{Re}\int_\delta \varphi_2$ is negative for a close to α. Now split σ into two stretches, the first one parametrized as $z(t) = z \circ \sigma(t) = -t$, $0 < t < x$, and the second $z(t) = t$, $0 < t < a$. If $\Sigma := \rho \circ \sigma$, then $Z \circ \Sigma(t) = z \circ \sigma(t)$. For the first stretch, from Figure 6 we have

$$g(\sigma(t)) = i|g(t)| = it^{\frac{1}{4}} \left(\frac{1 + at}{a + t}\right)^{\frac{1}{4}} \left(\frac{b + t}{1 + bt}\right)^{\frac{1}{2}} \left(\frac{x - t}{1 - xt}\right)^{\frac{1}{2}} \tag{17}$$

and

$$dh(t) = |dh(t)| = \frac{dt/t}{\sqrt{t + 1/t + a + 1/a}}. \tag{18}$$

For the second stretch,

$$g(\sigma(t)) = e^{\frac{i\pi}{4}}|g(t)| = e^{\frac{i\pi}{4}} t^{\frac{1}{4}} \left(\frac{1-at}{a-t}\right)^{\frac{1}{4}} \left(\frac{b-t}{1-bt}\right)^{\frac{1}{2}} \left(\frac{x+t}{1+xt}\right)^{\frac{1}{2}} \tag{19}$$

and

$$dh(t) = i|dh(t)| = \frac{dt/t}{\sqrt{t+1/t-a-1/a}}. \tag{20}$$

Thus $\operatorname{Re}\int_\sigma \varphi_2 = J_1 - J_2$, where

$$J_1 := \int_0^x \left(\frac{1}{|g|} - |g|\right)|dh| \quad \text{and} \quad J_2 := \frac{\sqrt{2}}{2}\int_0^a \left(\frac{1}{|g|} + |g|\right)|dh|. \tag{21}$$

The change $t = au$ shows that $\lim_{a\to 0} a^{-1/2} J_2$ exists and is finite. Regarding J_1, from (17) we shall have $1/|g| > |g|$ providing $(b+t)(x-t) < (1+bt)(1-xt)$. This last inequality is equivalent to $t^2 + 2(b-x)t/(1-bx) + 1 > 0$, which holds indeed, since $b - x > bx - 1$. Now, an easy computation shows that $\lim_{a\to 0} a^{-1/2} J_1 = +\infty$. We recall that $\operatorname{Re}\int_\sigma \varphi_2 = \operatorname{Re}\int_\delta \varphi_2$, and the latter is negative on (a, x_a), a close to α. These facts imply that there is a curve $\mathcal{C} \subset \text{graph}(b)$ such that both $\operatorname{Re}\int_\delta \varphi_2$ and $\operatorname{Re}\int_\gamma \varphi_2$ vanish simultaneously for every choice of $(a, b, x) \in \mathcal{C}$.

7 Refinements

In this section we study the curve $\mathcal{C}$ with more details. First of all, let us prove

Lemma 7.1. *There exists* $\lim_{a\to 0} x_a = 1$.

Proof. From (10), an easy computation shows that

$$\lim_{a\to 0} a^{-1/2} I_\gamma|_{b=1} = -\int_0^\pi \operatorname{Im}\left\{\sqrt{\frac{z+x}{xz+1}}\right\} dt. \tag{22}$$

The integral at (22) is negative for any $x \in (0,1)$, but converges to zero when x approaches 1. Since $\mathcal{R}$ is exactly the region where $I_\gamma|_{b=1}$ is non-positive, the same holds for this integral re-scaled by $a^{-1/2}$. Suppose there were a positive ε admitting a sequence $a_n \to 0$ with $x(a_n) < 1 - \varepsilon$ for all indexes n. In this case, the continuity of $a^{-1/2} I_\gamma|_{b=1}$, together with the fact that it is increasing with x, should give a non-negative limit in (22) for $x = 1 - \varepsilon$. This would be a contradiction. Therefore, we have $\lim_{a\to 0} x_a = 1$. □

In the remainder of this section, we prove that the curve $\mathcal{C}$ does not touch graph(x_a). Hence, it connects the point $(0,1,1)$ with some point of graph(b) over $(0,\alpha)\times\{0\} \ni (a,x)$. This will give a continuous one-parameter family of minimal surfaces with special limit-members. We shall describe them in Section 8.

From (1), if we put $b = 1$, this gives another family of compact Riemann surfaces R with algebraic equation

$$g^4 = z\left(\frac{1-az}{z-a}\right)\left(\frac{z+x}{xz+1}\right)^2. \tag{23}$$

Of course, (23) *cannot* be viewed as a limit of (1) for $b \to 1$. The algebraic equations describe abstract surfaces, not even contained in a metric space. Our only resource is the study of period integrals, of which some limits can converge to integrals on another compact surface.

The surfaces in (23) are endowed with the following involution: $(z, g) \to (z, ig)$. Since $i^4 = 1$, there are exactly four points of branch order 3, namely $(0, 0)$, $(1/a, 0)$, (a, ∞) and (∞, ∞). Moreover, there remain only four other branch points, $(-x, \pm 0)$ and $(-1/x, \pm\infty)$, these of order 1. Here the $\pm$ signs indicate different *germs* of functions. The Riemann–Hurwitz formula gives

$$\frac{4 \cdot 3 + 4 \cdot 1}{2} - 4 + 1 = 5.$$

From now on, our analysis will be strongly based in [16]. There one proves that the algebraic equations

$$\left(G + \frac{1}{G}\right)^2 = \frac{4\zeta(\zeta - y)^2(\zeta - 1/\lambda)}{(\zeta^2 - 1)(\zeta - \kappa)(\zeta - 1/\kappa)} \tag{24}$$

and

$$\left(G - \frac{1}{G}\right)^2 = \frac{4(1 - y\zeta)^2(1 - \zeta/\lambda)}{(\zeta^2 - 1)(\zeta - \kappa)(\zeta - 1/\kappa)} \tag{25}$$

are equivalent if and only if $\lambda(\kappa + 1/\kappa) = 1 + (2\lambda - y)y$, with $2\lambda - 1 < y < \lambda < \kappa < 1$ and positive λ. Moreover, the Riemann surfaces M defined by (24-5) have genus 5. Notice that M is endowed with the involution $\imath$ given by $(\zeta, G) \to (1/\zeta, iG)$.

From [16, pp. 351–353] one has that ζ is the pull-back under $\imath^2$ of an elliptic function $\mathcal{Z}$ defined on a rectangular torus $\mathcal{T}$. The parameter λ can freely vary in $(0, 1)$, describing all rectangular tori. From Section 3 and [16, pp. 352], one sees that the choice $a = \lambda$ makes $T = \mathcal{T}$ and Z a "shift" of $\mathcal{Z}$. By defining $\Lambda := \lambda + 1/\lambda$, the following relation holds:

$$\left(\frac{Z+1}{Z-1}\right)^2 = \frac{\mathcal{Z} + 1/\mathcal{Z} - \Lambda}{2 - \Lambda}. \tag{26}$$

If we choose $\mathcal{Z} = \kappa$, a unique $Z(\kappa) \in (-1, 0)$ will be determined by (26). So we take $a = \lambda$ and $x = -Z(\kappa)$ in (23).

Let $\boldsymbol{z}$ be the pull-back of Z under $\imath^2$. Therefore, $\boldsymbol{z}((1, 0)) = 0$, $\boldsymbol{z}((1, \infty)) = \infty$, $\boldsymbol{z}((-1, \infty)) = a$ and $\boldsymbol{z}((-1, 0)) = 1/a$, while $\boldsymbol{z}((\kappa^{\pm 1}, 0)) = -x$ and $\boldsymbol{z}((\kappa^{\pm 1}, \infty)) = -1/x$. Let ℓ_j be a single small loop in $\mathbb{C}$ around 0, a, $1/a$, $-x$ and $-1/x$, for $j = 1, \ldots, 5$, respectively. We take lifts $\hat{\ell}_j$ of ℓ_j by $\boldsymbol{z}$ and notice that the end points of $\hat{\ell}_j$ differ by $\imath^{k_j}$, $0 \le k_j \le 3$, $1 \le j \le 5$.

Let D be the open unitary complex disk at the origin. Since $deg(\boldsymbol{z}) = 4$, there is a coordinate chart $w : D \to M$ with $w(0) = (1, 0)$ such that $\boldsymbol{z}(w) = w^4$. By taking ℓ_1

small enough to be in $\boldsymbol{z}(w(D))$, we conclude that $k_1 = 1$. The same reasoning will give $k_2 = -k_3 = -1$. If we had taken $w(0) = (\kappa, 0)$, then $\boldsymbol{z}(w) = c_1 + w^2$ and so $k_4 = 2$. By the same reasoning $k_5 = -2$. Let us define $\mathcal{A} := \mathbb{C} \setminus \{0, a^{\pm 1}, -x^{\pm 1}\}$.

The numbers k_j naturally determine a homomorphism $H : \pi_1(\mathcal{A}) \to \mathbb{Z}_4 \oplus \mathbb{Z}_2$, of which the kernel is $\boldsymbol{z}_*(\pi_1(M \setminus \{(\pm 1, 0^{\pm 1}), (\kappa^{\pm 1}, 0^{\pm 1})\})) \subset \pi_1(\mathcal{A})$. By going back to (23), one sees that the projection map $z : R \to \hat{\mathbb{C}}$, namely $(z, g) \to z$, is such that $z_*(\pi_1(R \setminus g^{-1}(\{0, \infty\})))$ also represents the kernel of H. From [11, p. 159], there is a fiber-preserving biholomorphism $\beta : M \to R$ such that $\boldsymbol{z} = z \circ \beta$. As a matter of fact, that reference treats unbranched coverings, but the conclusion still applies to our case.

From [16] and the above paragraph, one sees that G^4 has the same divisor as $\boldsymbol{z}(1 - a\boldsymbol{z})/(\boldsymbol{z} - a) \cdot [(\boldsymbol{z} + x)/(x\boldsymbol{z} + 1)]^2$. By composing $\boldsymbol{z}$ with the involution $(\zeta, G) \to (\bar{\zeta}, 1/\bar{G})$ we get $\boldsymbol{z} \to 1/\bar{\boldsymbol{z}}$. Therefore, G is unitary where $\boldsymbol{z}$ is. Now, by composing $\boldsymbol{z}$ with the involution $(\zeta, G) \to (1/\bar{\zeta}, i\bar{G})$ we get $\boldsymbol{z} \to \bar{\boldsymbol{z}}$. This means that $|\zeta| = 1$ implies $\boldsymbol{z}^{\pm 1} \in (0, a)$. Hence

$$G^4 = \boldsymbol{z}\left(\frac{1 - a\boldsymbol{z}}{\boldsymbol{z} - a}\right)\left(\frac{\boldsymbol{z} + x}{x\boldsymbol{z} + 1}\right)^2,$$

and so we can take $G = g \circ \beta$. In [16] one defines dH as the pull-back of the holomorphic differential form on T. As we have already mentioned, ζ is the pull-back of $\mathcal{Z}$, which is a shift of Z. Hence, the pull-back of $\mathcal{Z}'/\mathcal{Z}$ gives a well-defined square-root of $\boldsymbol{z} + 1/\boldsymbol{z} - a - 1/a$ on M, and so dH is proportional to $\boldsymbol{z}^{-1} d\boldsymbol{z}/\sqrt{\boldsymbol{z} + 1/\boldsymbol{z} - a - 1/a}$. But since dH is purely imaginary for $|\boldsymbol{z}| = 1$, the proportional constant must be $\pm i$. The sign just changes the minimal immersion to its antipodal, so we take

$$dH = \frac{i d\boldsymbol{z}/\boldsymbol{z}}{\sqrt{\boldsymbol{z} + 1/\boldsymbol{z} - a - 1/a}}.$$

From Proposition 8.1 of [16], or even better [15], and the above discussion, one sees that each $a \in (0, 1)$ admits a *unique* $\boldsymbol{x}$ for which $\operatorname{Re} \int_{\boldsymbol{\sigma}} \boldsymbol{\phi}_2 = 0$. Now suppose that $\mathcal{C} \cap \operatorname{graph}(x_a) \neq \emptyset$. In this case, there is $\mathtt{a} \in (0, \alpha)$ such that $\operatorname{Re} \int_\delta \varphi_2 = \operatorname{Re} \int_\sigma \varphi_2 = 0$ for $(a, b, x) = (\mathtt{a}, 1, x_{\mathtt{a}})$. Therefore, it exists $\varepsilon > 0$ such that $\operatorname{Re} \int_\delta \varphi_2 = 0$ for all $(a, b, x) \in B_\varepsilon(\mathtt{a}, 1, x_{\mathtt{a}}) \cap \mathcal{C}$.

Back to (13) and (14), the change $t \mapsto b - t^2$ shows that

$$\lim_{b \to 1} \operatorname{Re} \int_\delta \varphi_2 = \operatorname{Re} \int_a^1 \boldsymbol{\phi}_2.$$

From the uniqueness, $\boldsymbol{x} = x_{\mathtt{a}}$ because $\operatorname{Re} \int_{\boldsymbol{\sigma}} \boldsymbol{\phi}_2 = \operatorname{Re} \int_\sigma \varphi_2|_{b=1}$ and the latter is zero at $(\mathtt{a}, 1, x_{\mathtt{a}}) \in \mathcal{C}$. But in [16] one proves that such a choice gives an embedded surface, and in particular $\operatorname{Re} \int_a^1 \boldsymbol{\phi}_2$ is *negative*.

Therefore, if ε is close enough to zero, then $\operatorname{Re} \int_\delta \varphi_2$ must be negative in $B_\varepsilon(\mathtt{a}, 1, x_{\mathtt{a}})$, a contradiction. We conclude that $\mathcal{C} \cap \operatorname{graph}(x_a) = \emptyset$. Consequently, the curve $\mathcal{C}$ connects $(a, b, x) = (0, 1, 1)$ with $(a, b, x) = (a^*, b^*, 0)$, for a certain $a^* \in (0, \alpha)$ and $b^* = b(a^*, 0)$.

8 Limits and embeddedness

At this point we have proved all but one item of Theorem 1.1. This last section is devoted to its accomplishment. By lopping off occasional loops of $\mathcal{C}$, we consider it a simple curve. Let $s \mapsto (a(s), b(s), x(s))$ be a monotone parametrization of $\mathcal{C}$, assuming $(0, 1, 1)$ at $s = 0$ and $(a^*, b^*, 0)$ at $s = 1$. For every $s \in (0, 1)$, we have a well-defined minimal immersion $X_s : \bar{S} \to \mathbb{R}^3/G$, determined by (g, dh) at (1) and (4).

Now consider u as a complex variable of $\hat{\mathbb{C}}$ and take $z = au/(u-1)$ in (1) and (4). If K is a compact subset of $\hat{\mathbb{C}} \setminus \{1\}$, for $u \in K$ a simple computation gives

$$\lim_{s\to 0} g^4 = u \quad \text{and} \quad \lim_{s\to 0} \frac{dh}{\sqrt{a}} = \frac{4dg/g}{g^2 - 1/g^2}. \tag{27}$$

One readily recognizes (27) as the Weierstrass data of Scherk's doubly periodic surface. Namely, the coordinates of the minimal immersion X_s converge uniformly in K to Scherk's coordinates. More precisely, suppose that K is the 4^{th}-power image of a compact $\mathsf{K} \subset \hat{\mathbb{C}} \setminus \{\pm 1, \pm i\}$. In this set, g is the standard complex coordinate, which together with $gdg/(g^4 - 1)$ gives the classical Scherk's doubly periodic surface. Figure 8 shows how the surface looks like for a close to zero.

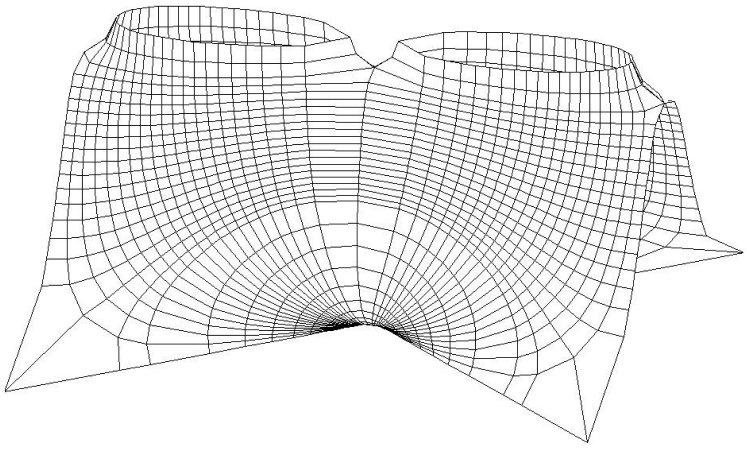

Figure 8. The case $(a, b, x) = (0.15, 0.8, 0.74)$.

Consider now z as the complex variable of $\hat{\mathbb{C}}$ and define $\mathsf{D} := \{z \in \mathbb{C} : |z| < 1 < 1 + \mathrm{Im}\{z\}\}$. For z in a compact $\boldsymbol{K} \subset \mathsf{D} \setminus \{0\}$, one immediately gets

$$\lim_{s\to 1} g^4 = z^3 \left(\frac{1 - a^* z}{z - a^*}\right)\left(\frac{b^* - z}{b^* z - 1}\right)^2, \tag{28}$$

while $\lim_{s\to 1} dh$ is given by (4) with $a = a^*$. From [17, Section 7] we recognize the Weierstrass data of a genus 5 example from Hoffman–Wohlgemuth. In fact, to date there

is just numerical evidence that each genus $4k+1$ gives a *unique* Hoffman–Wohlgemuth surface, $k \in \mathbb{N}^*$. However, in [17] one gets all such surfaces from the *intermediate value theorem*. The choice $(a,b) = (a^*,b^*)$ is then included in [17], since our surfaces are period free for all $s \in (0,1)$.

Finally, the same arguments from [16, pp. 360–362] imply that X_s is in fact an embedding, for any $s \in (0,1)$. Figure 9 illustrates what happens for s close to 1. Figure 1 shows the fundamental piece for $(a,b,x) = (0.47, 0.85, 0.68)$.

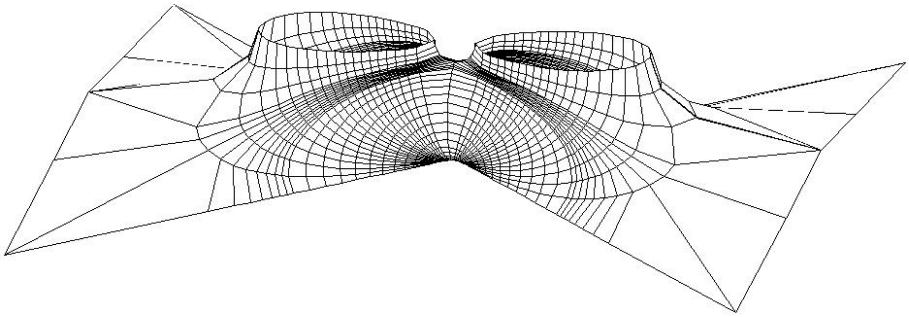

Figure 9. The case $(a,b,x) = (0.65, 0.89, 0.69)$.

We conclude this last section with the demonstration of Corollary 1.1. For the Weierstrass data of the Hoffman–Wohlgemuth surface, dh is the same as in (4), and g is given by (28), so that we have a surface of genus 5 with two planar ends, namely at $z=0$ and $z=\infty$. Moreover, dh gives a non-zero integral along $a < z < 1/a$. This means that the two planar ends are disjoint. Such ends are graphs, hence embedded.

Therefore, if the Hoffman–Wohlgemuth surface had a self-intersection, it would be in a ball of $\mathbb{R}^3$. By the *maximum principle* for minimal surfaces, the same would happen to X_s, for s close enough to 1. But from Theorem 1.1, we know that X_s is embedded for all $s \in (0,1)$.

References

[1] M. Callahan, D. Hoffman, W. H. Meeks, III, Embedded minimal surfaces with an infinite number of ends. *Invent. Math.* **96** (1989), 459–505. MR996552 (90b:53005) Zbl 0676.53004

[2] L. Hauswirth, J. Pérez, P. Romon, Embedded minimal ends of finite type. *Trans. Amer. Math. Soc.* **353** (2001), 1335–1370. MR1806738 (2002b:53003) Zbl 0986.53005

[3] D. Hoffman, H. Karcher, Complete embedded minimal surfaces of finite total curvature. In: *Geometry, V*, volume 90 of *Encyclopaedia Math. Sci.*, 5–93, 267–272, Springer 1997. MR1490038 (98m:53012) Zbl 0890.53001

[4] D. Hoffman, H. Wohlgemuth, New embedded periodic minimal surfaces of Riemann-type. Manuscript, 1993.

[5] H. Karcher, Embedded minimal surfaces derived from Scherk's examples. *Manuscripta Math.* **62** (1988), 83–114. MR958255 (89i:53009) Zbl 0658.53006

[6] H. Karcher, Construction of minimal surfaces. Lecture Notes 12, SFB256, Bonn, 1989.

[7] H. Karcher, The triply periodic minimal surfaces of Alan Schoen and their constant mean curvature companions. *Manuscripta Math.* **64** (1989), 291–357. MR1003093 (90g:53010) Zbl 0687.53010

[8] H. Karcher, F. S. Wei, D. Hoffman, The genus one helicoid and the minimal surfaces that led to its discovery. In: *Global analysis in modern mathematics* (*Orono, ME,* 1991*; Waltham, MA,* 1992), 119–170, Publish or Perish, Houston, TX 1993. MR1278754 (95k:53011) Zbl 1049.53502

[9] F. J. López, F. Martín, Complete minimal surfaces in $\mathbf{R}^3$. *Publ. Mat.* **43** (1999), 341–449. MR1744617 (2002c:53010) Zbl 0951.53001

[10] F. Martín, D. Rodríguez, A characterization of the periodic Callahan-Hoffman-Meeks surfaces in terms of their symmetries. *Duke Math. J.* **89** (1997), 445–463. MR1470339 (98h:53016) Zbl 0901.53006

[11] W. S. Massey, *Algebraic topology: An introduction*. Harcourt, Brace & World, Inc., New York 1967. MR0211390 (35 #2271) Zbl 0153.24901

[12] J. C. C. Nitsche, *Lectures on minimal surfaces. Vol.* 1. Cambridge Univ. Press 1989. MR1015936 (90m:49031) Zbl 0688.53001

[13] R. Osserman, *A survey of minimal surfaces*. Dover Publications Inc., New York 1986. MR852409 (87j:53012) Zbl 0209.52901

[14] J. Pérez, M. M. Rodríguez, M. Traizet, The classification of doubly periodic minimal tori with parallel ends. *J. Differential Geom.* **69** (2005), 523–577. MR2170278 (2006j:53010) Zbl 1094.53007

[15] V. Ramos Batista, Theoretical evaluation of elliptic integrals based on computer graphics. Technical Report 71/02, Campinas 2002. http://www.ime.unicamp.br/rel_pesq/2002/rp71-02.html

[16] V. Ramos Batista, A family of triply periodic Costa surfaces. *Pacific J. Math.* **212** (2003), 347–370. MR2038053 (2005a:53011) Zbl 1059.53013

[17] V. Ramos Batista, P. Simões, A characterisation of the Hoffman-Wohlgemuth surfaces in terms of their symmetries. *Geom. Dedicata* **142** (2009), 191–214. Zbl pre05614996

[18] M. Weber, D. Hoffman, M. Wolf, The genus-one helicoid as a limit of screw-motion invariant helicoids with handles. In: *Global theory of minimal surfaces*, volume 2 of *Clay Math. Proc.*, 243–258, Amer. Math. Soc. 2005. MR2167262 (2006f:53015) Zbl 1102.53008

Received 7 April, 2008; revised 4 May, 2009

P. Simões, IME - University of São Paulo, rua do Matão 1010, 05508-090 São Paulo-SP, Brazil
Email: paqs@ime.usp.br

V. Ramos Batista, Universidade Federal do ABC, rua Catequese 242, 3o. andar, 09090-400 Santo André-SP, Brazil
Email: valerio.batista@ufabc.edu.br